

Electronic Supplementary Information for

Highly Selective Detecting antibiotics and Noble Metal Catalyst Support by a Multifunctional
Eu-MOF

Bo Li^a, Yu-Ying Jiang^{a,b}, Ya-Ya Sun^a, Yan-Jiang Wang^a, Min-Le Han^{*,b} Ya-Pan Wu^a, Lu-Fang Ma^b, and
Dong-Sheng Li^{*,a}

^a College of Materials & Chemical Engineering, Collaborative Innovation Centre for Microgrid of
New Energy of Hubei Province, Key laboratory of inorganic nonmetallic crystalline and energy
conversion materials, China Three Gorges University, Yichang, 443002, China. Tel./Fax:
+86-717-6397506; E-mail address: lidongsheng1@126.com (D.-S. Li).

^b College of Chemistry and Chemical Engineering, and Henan Key Laboratory of Function-Oriented
Porous Materials, Luoyang Normal University, Luoyang 471934, P. R. China. E-mail address:
minle_han@163.com (M.-L. Han).

Table of Contents

1. Table S1. The selected bond lengths [Å] and angles [°] of complex **CTGU-19**.
2. Figure S1. The channel width of **CTGU-19**.
3. Figure S2. The powder X-ray diffraction pattern of **CTGU-19** are immersed in different pH solutions for 24 h.
4. Figure S3. The PXRD was obtained after **CTGU-19** was immersed in 0.2mM different antibiotic solutions for 48h.
5. Figure S4. TGA curves for **CTGU-19** under air atmosphere.
6. Figure S5. Excitation and emission spectra for **CTGU-19**.
7. Figure S6. Fluorescence spectrum of **CTGU-19** dispersed in aqueous solutions of different concentrations of antibiotics under (a) 320 nm; (b) 359 nm excitation.
8. Figure S7. (a) The plot of $I_0/I - 1$ of **CTGU-19** in different concentration of ODZ solution. (b) The plot of $I_0/I - 1$ of **CTGU-19** in different concentration of NFT solution.
9. Figure S8. Fluorescence intensity of CTGU-19 by different antibiotics at room temperature and selective detection of (a) ODZ; (b)NFT in water.
10. Figure S9. Uv-vis absorption spectra of different antibiotic solutions.
11. Table S2. Element content in composite catalyst.
12. Figure S10. The energy dispersive X-ray (EDX) spectroscopy analysis of (a) Ag@**CTGU-19**; (b) Au@**CTGU-19**; (c) Ag_{0.8}-Au_{0.2}@**CTGU-19**.
13. Figure S11. The catalytic reduction 4-NP and the plot of $\ln(C_t/C_0) \sim t$ of Ag_{0.1}-Au_{0.9}@**CTGU-19** (a), Ag_{0.2}-Au_{0.8}@**CTGU-19** (b), Ag_{0.3}-Au_{0.7}@**CTGU-19** (c); Ag_{0.4}-Au_{0.6}@**CTGU-19** (d), Ag_{0.5}-Au_{0.5}@**CTGU-19** (e), Ag_{0.6}-Au_{0.4}@**CTGU-19** (f), Ag_{0.7}-Au_{0.3}@**CTGU-19** (g) and Ag_{0.9}-Au_{0.1}@**CTGU-19** (h).
14. Figure S12. Relationship between In (C_t/C_0) and reaction time (t) of 4-NP in **CTGU-19** catalytic reduction with different silver nitrate loads.
15. Table S3. The catalytic activity of 0.1mg composite catalyst for 4-NP reduction reaction.
16. Table S4. The catalytic activity of 0.2mg composite catalyst for 4-NP reduction reaction.

- 17.** Table S5. Catalytic activity of composite catalyst for 4-NP reduction reaction.
- 18.** Figure S13. PXRD of (a) Ag@**CTGU-19**; (b) Au@**CTGU-19**; (c) Ag_{0.8}-Au_{0.2}@**CTGU-19** before and after nitrophenol reduction experiment.
- 19.** Figure S14. Five cycles of Ag_{0.8}-Au_{0.2}@**CTGU-19** reduction of 4-NP.
- 20.** Table S6. Summary of rate constants of other similar 4-nitrophenol reduction reactions catalyzed by previously reported catalysts.
- 21.** Table S7. Summary of rate constants of other similar 2-nitrophenol reduction reactions catalyzed by previously reported catalysts.
- 22.** Table S8. Summary of rate constants of other similar 3-nitrophenol reduction reactions catalyzed by previously reported catalysts.

Table S1. The selected bond lengths [Å] and angles [°] of complex **CTGU-19**.

Eu1-O1	2.384(2)	Eu1-O3#3	2.406(2)
Eu1-O2#3	2.404(3)	Eu1-O4#5	2.387(2)
Eu1-O3	2.364(2)	Eu1-O5#4	2.446(2)
Eu1-O3#1	2.384(2)	Eu1-N1#5	2.593(3)
O1-Eu1-O5#4	78.17(8)	O3#2-Eu1-O2#1	78.84(9)
O1-Eu1-O3#1	73.68(8)	O3-Eu1-O4#5	108.19(8)
O1-Eu1-O4#5	144.57(8)	O3#2-Eu1-O4#5	71.69(8)
O1-Eu1-O2#1	97.13(10)	O3-Eu1-O3#1	69.71(8)
O1-Eu1-N1#5	80.53(9)	O3-Eu1-O3#2	69.08(9)
O2#1-Eu1-N1#5	79.20(9)	O3#2-Eu1-O3#1	69.38(8)
O2#1-Eu1-O3#1	79.24(8)	O3-Eu1-O5#4	68.76(8)
O2#1-Eu1-O5#4	149.80(9)	O3#2-Eu1-O5#4	122.51(8)
O3#1-Eu1-N1#5	143.77(8)	O3#1-Eu1-O5#4	126.27(8)
O3#2-Eu1-N1#5	133.21(9)	O4#5-Eu1-O5#4	86.49(8)
O3-Eu1-N1#5	139.07(9)	O4#5-Eu1-O3#2	138.75(8)
O3-Eu1-O1	95.78(9)	O4#5-Eu1-O2#1	80.41(9)
O3#2-Eu1-O1	142.96(7)	O4#5-Eu1-N1#5	64.22(9)
O3-Eu1-O2##1	141.28(8)	O5#4-Eu1-N1#5	70.61(8)

Symmetry code: #1 1-X,3/2-Y,+Z; #2 -1/4+Y,5/4-X,5/4-Z; #3 5/4-Y,1/4+X,5/4-Z; #4 3/4-Y,1/4+X,-3/4+Z;

#5 1-X,1-Y,1-Z; #6 -1/4+Y,3/4-X,3/4+Z

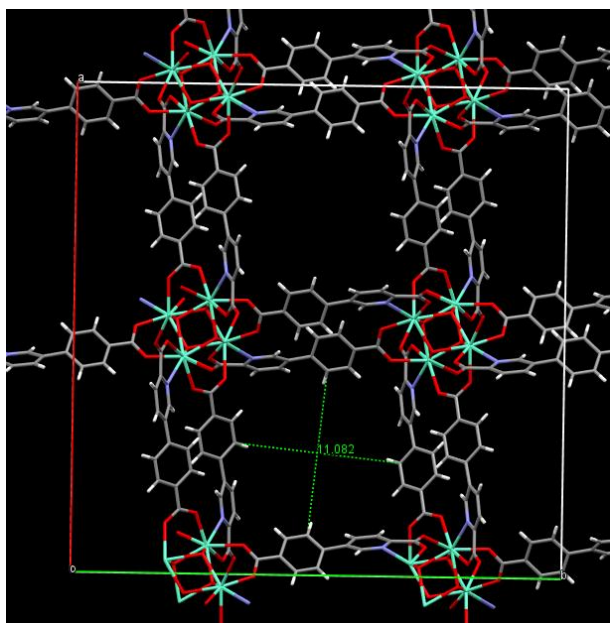


Figure S1. The channel width of **CTGU-19**.

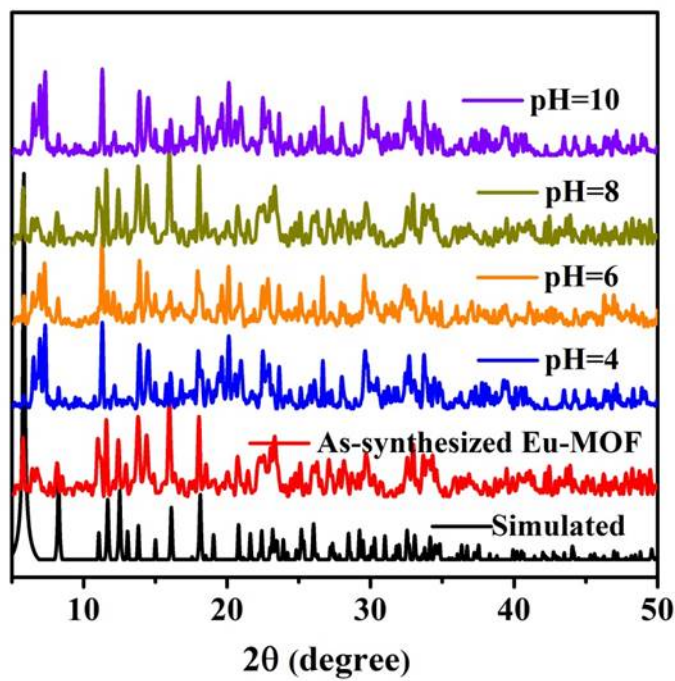


Figure S2. The powder X-ray diffraction pattern of **CTGU-19** are immersed in different pH solutions for 24 h.

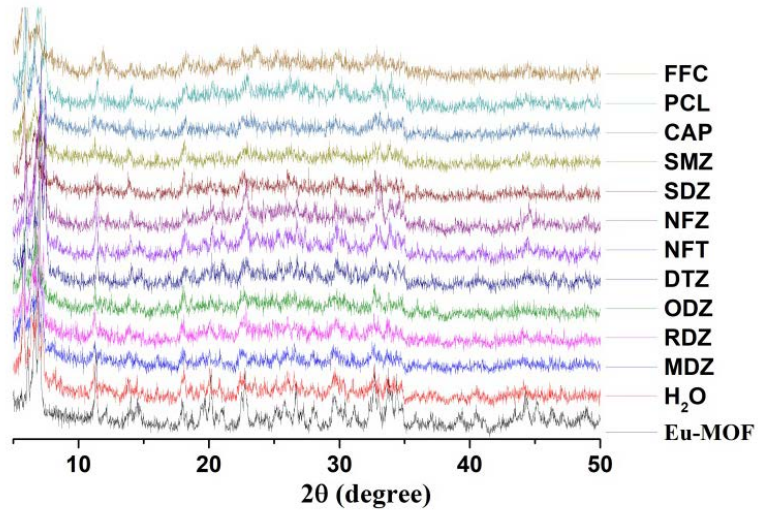


Figure S3. The PXRD was obtained after **CTGU-19** was immersed in 0.2mM different antibiotic solutions for 48h.

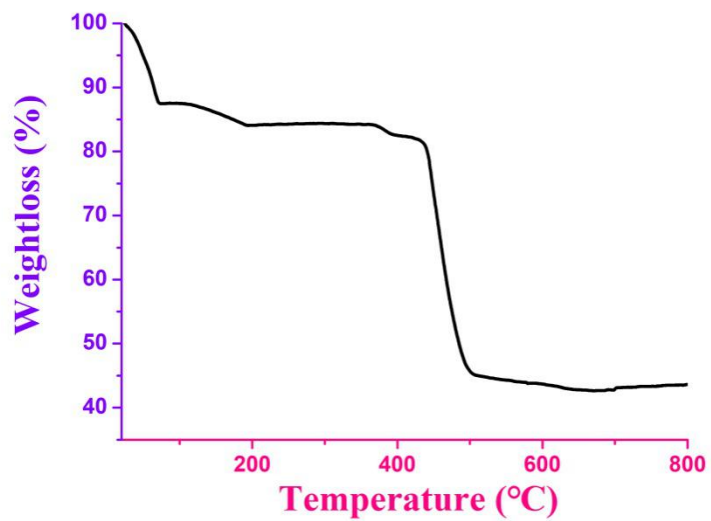
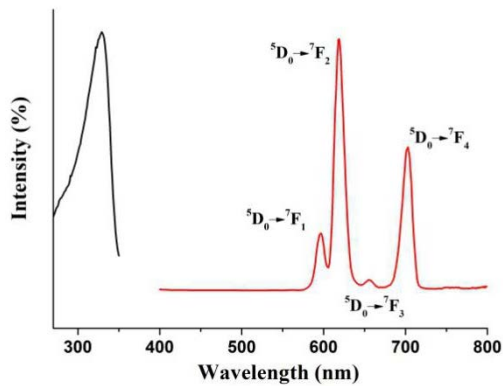
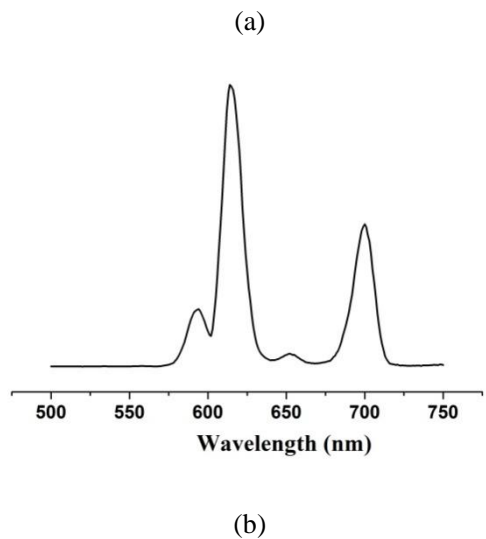


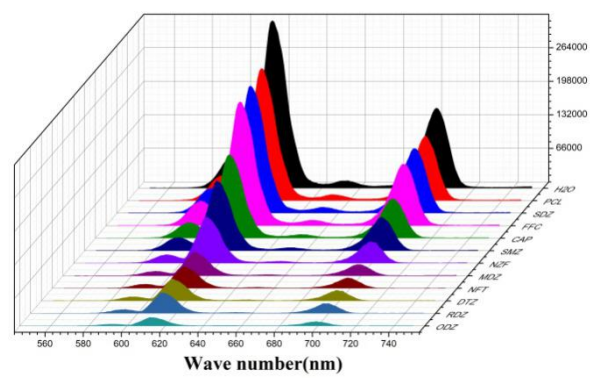
Figure S4. TGA curves for **CTGU-19** under air atmosphere.



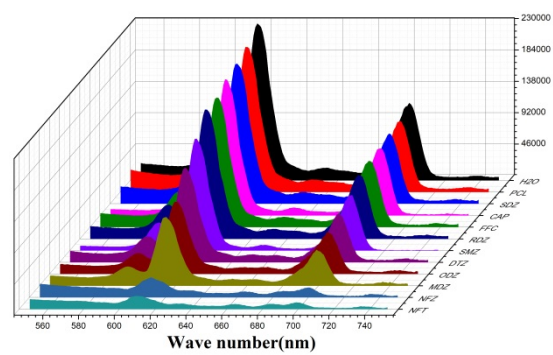


(b)

Figure S5. (a) Solid-state excitation and emission spectra for **CTGU-19** at room temperature. (b) Liquid excitation and emission spectra of **CTGU-19** at room temperature.

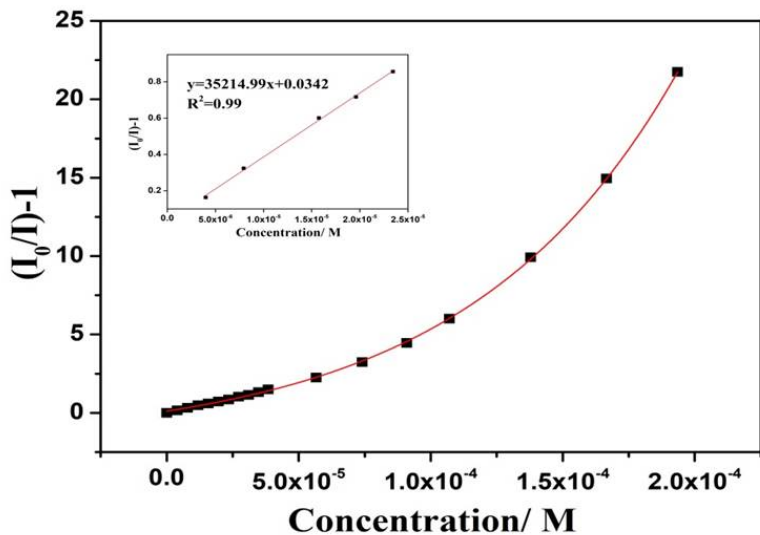


(a)

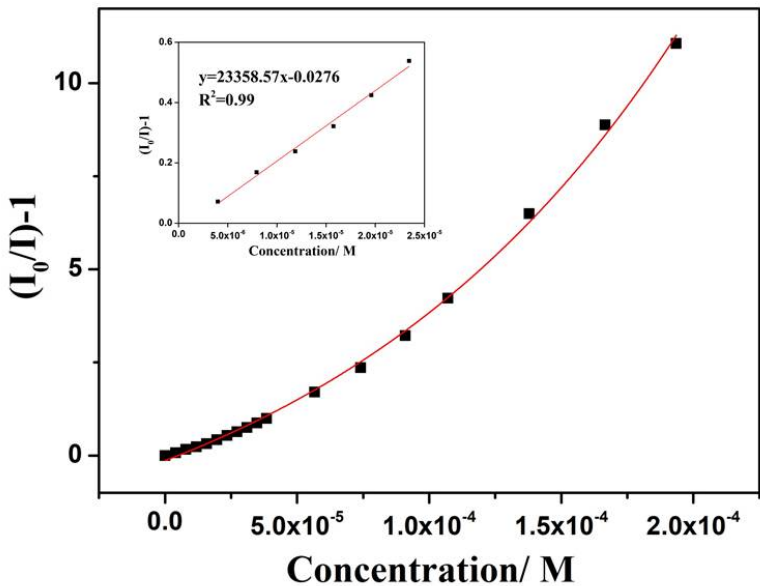


(b)

Figure S6. Fluorescence spectrum of **CTGU-19** dispersed in aqueous solutions of different antibiotics under (a) 320nm; (b) 359nm excitation

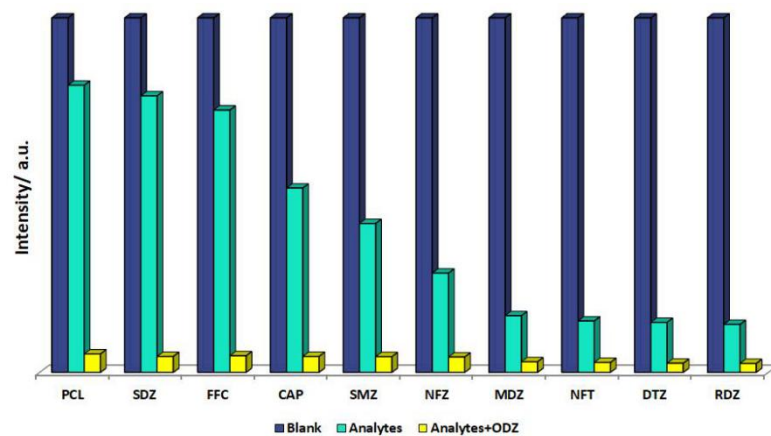


(a)

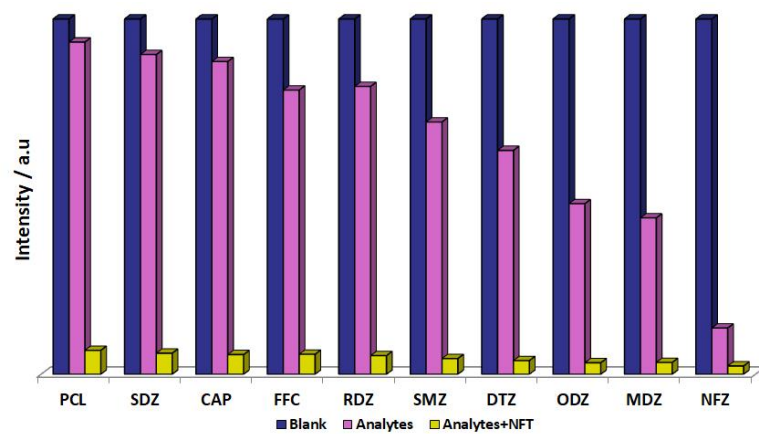


(b)

Figure S7. (a) The plot of $I_0/I - 1$ of **CTGU-19** in different concentration of ODZ solution. (b) The plot of $I_0/I - 1$ of **CTGU-19** in different concentration of NFT solution.



(a)



(b)

Figure S8. Fluorescence intensity of CTGU-19 by different antibiotics at room temperature and selective detection of (a) ODZ; (b)NFT in water.

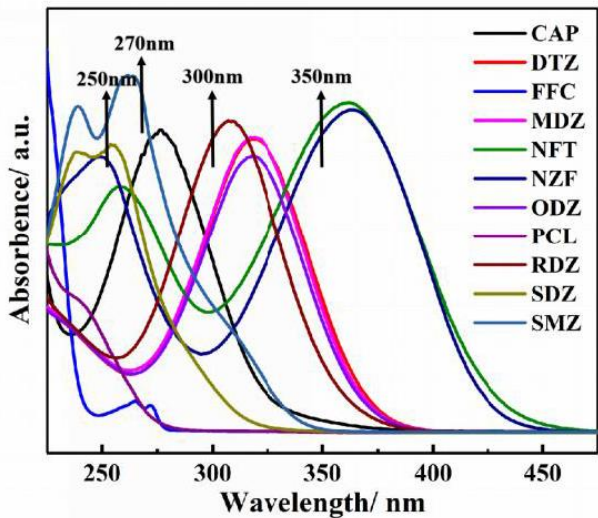
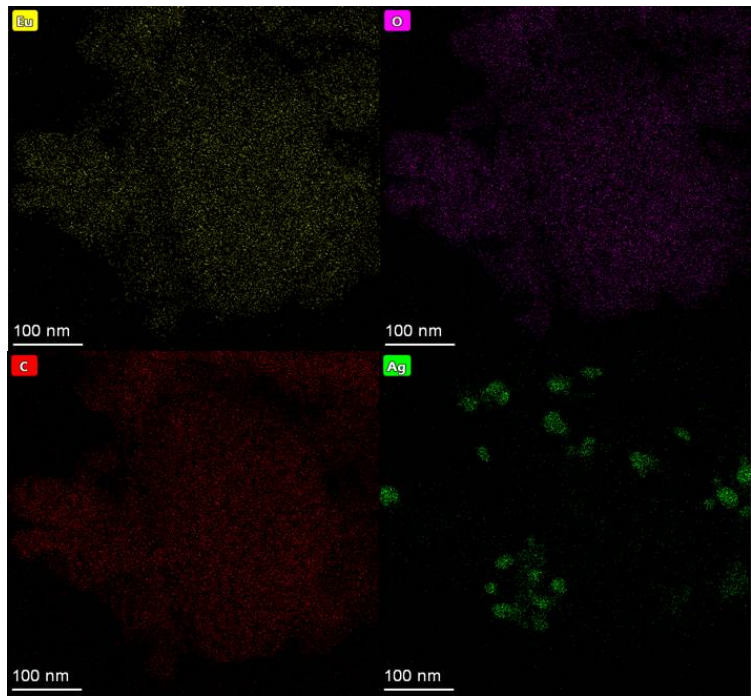


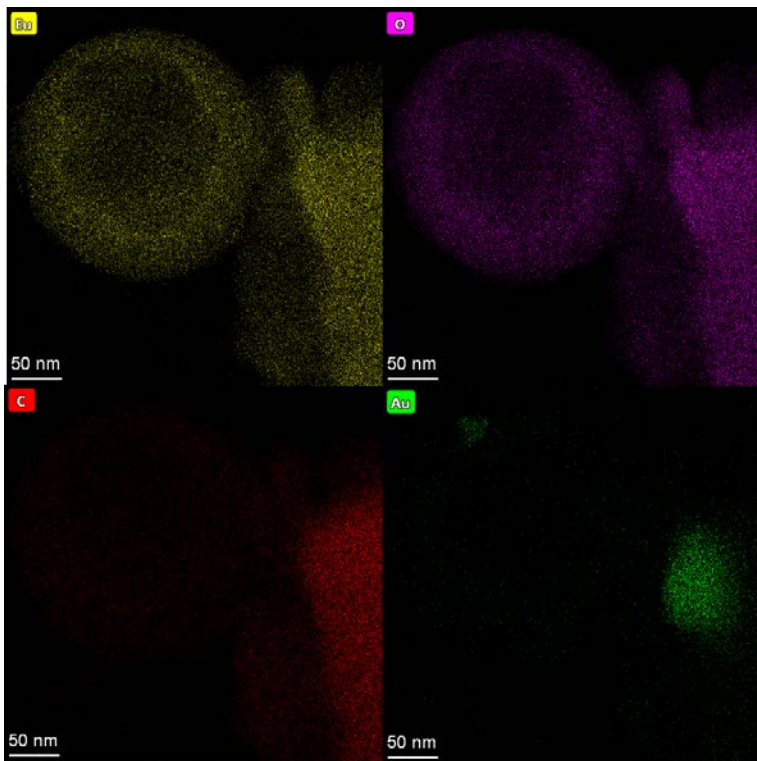
Figure S9. Uv-vis absorption spectra of different antibiotic solutions.

Table S2. Element content in composite catalyst.

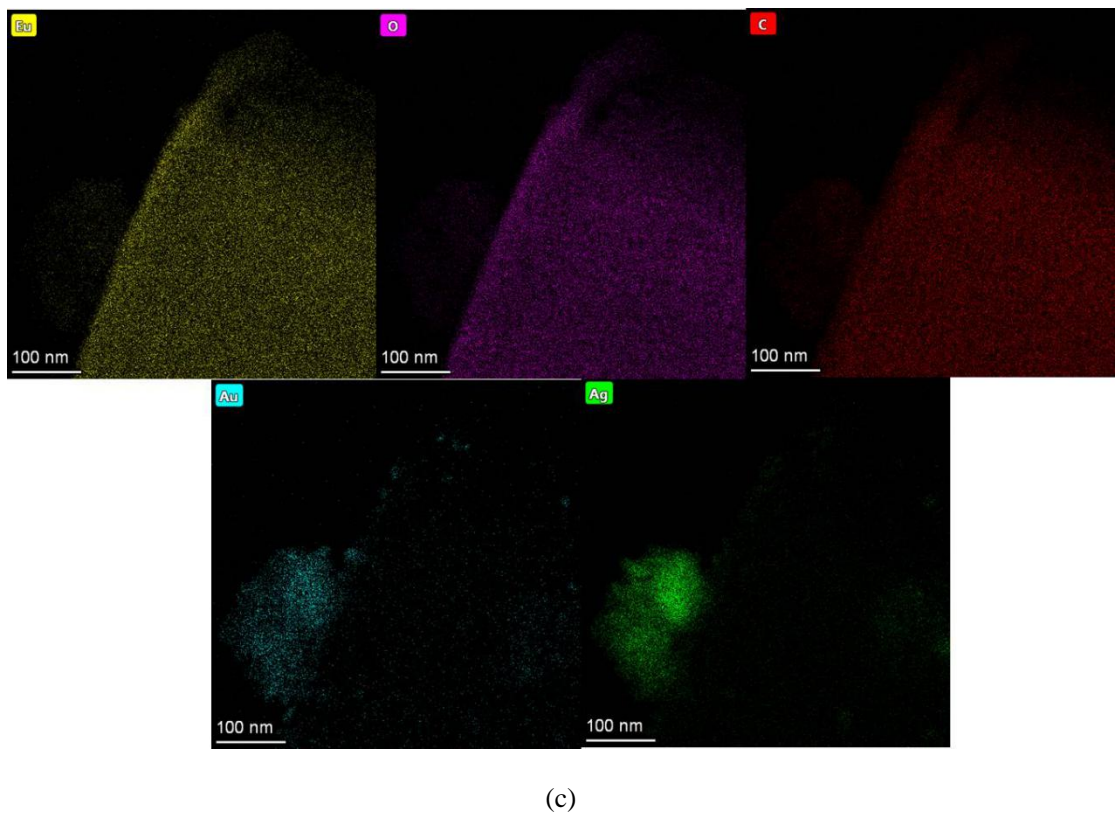
Ag@CTGU-19	Ag	0.85%
	Eu	33.73%
Au@CTGU-19	Au	0.94%
	Eu	27.67%
Ag_{0.2}-Au_{0.8}@CTGU-19	Au	4.60%
	Ag	4.14%
	Eu	23.45%



(a)

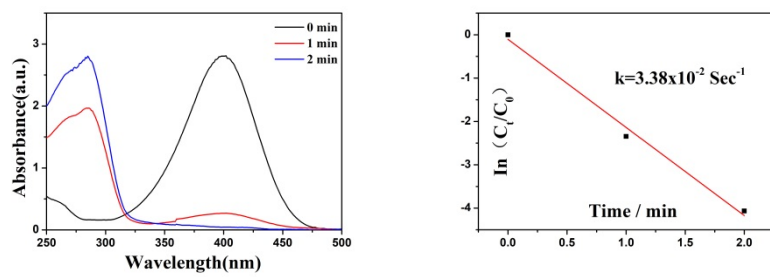


(b)

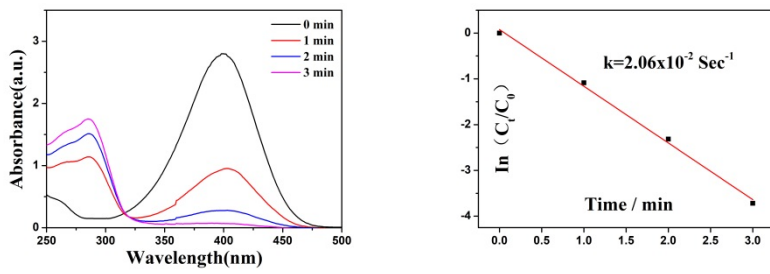


(c)

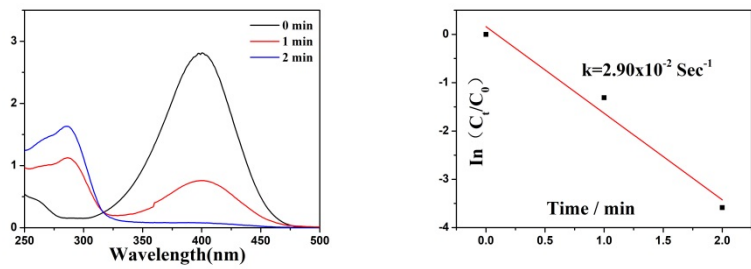
Figure S10. The energy dispersive X-ray (EDX) spectroscopy analysis of (a) Ag@CTGU-19; (b) Au@CTGU-19; (c) Ag_{0.8}-Au_{0.2}@CTGU-19.



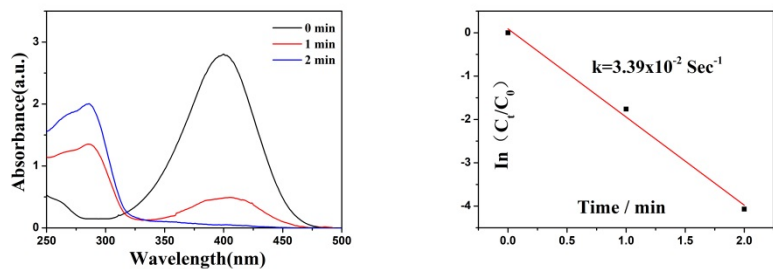
(a)



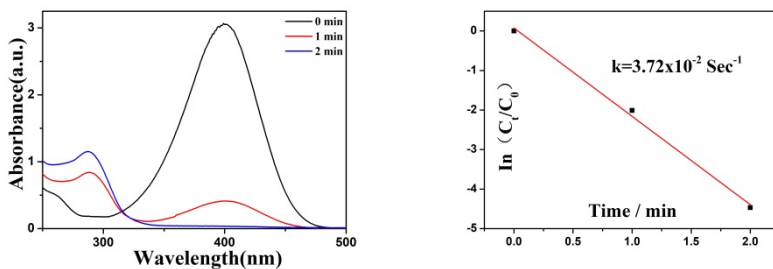
(b)



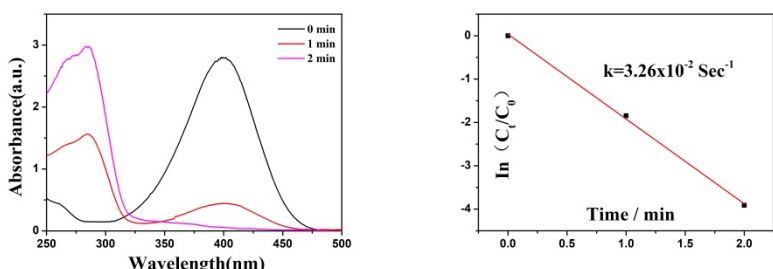
(c)



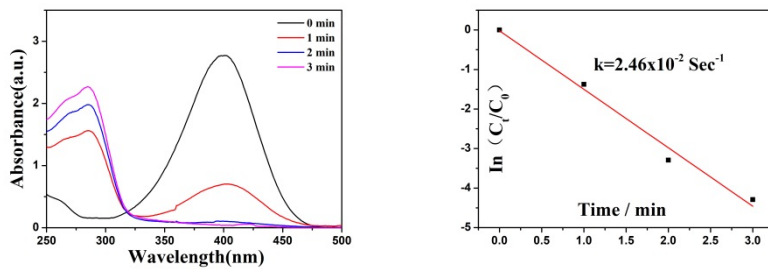
(d)



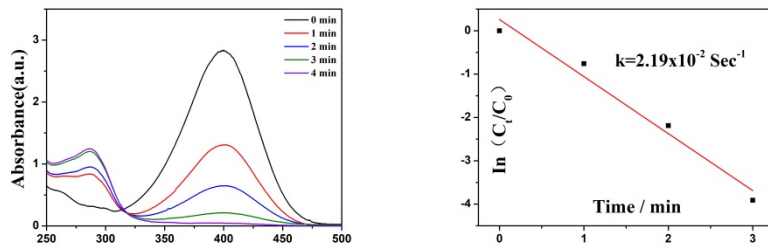
(e)



(f)



(g)



(h)

Figure S11. The catalytic reduction 4-NP and the plot of $\ln(C_t/C_0) \sim t$ of **Ag_{0.1}-Au_{0.9}@CTGU-19** (a), **Ag_{0.2}-Au_{0.8}@CTGU-19** (b), **Ag_{0.3}-Au_{0.7}@CTGU-19** (c); **Ag_{0.4}-Au_{0.6}@CTGU-19** (d), **Ag_{0.5}-Au_{0.5}@CTGU-19** (e), **Ag_{0.6}-Au_{0.4}@CTGU-19** (f), **Ag_{0.7}-Au_{0.3}@CTGU-19** (g) and **Ag_{0.9}-Au_{0.1}@CTGU-19** (h).

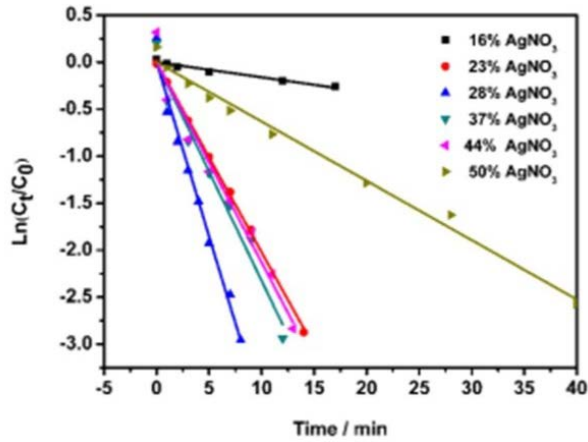


Figure S12. Relationship between $\ln(C_t/C_0)$ and reaction time (t) of 4-NP in **CTGU-19** catalytic reduction with different silver nitrate loads.

Table S3. The catalytic activity of 0.1 mg composite catalyst for 4-NP reduction reaction.

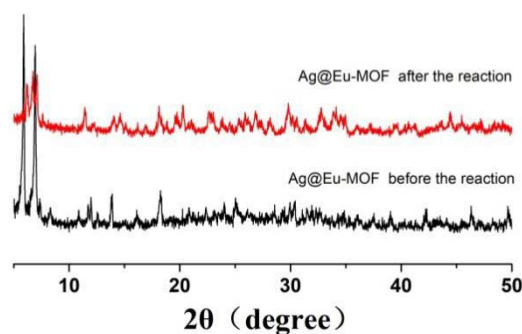
Ag@CTGU-19	93.67 s ⁻¹ .g ⁻¹
Ag_{0.9}-Au_{0.1}@CTGU-19	78 s ⁻¹ .g ⁻¹
Ag_{0.8}-Au_{0.2}@CTGU-19	298 s ⁻¹ .g ⁻¹
Ag_{0.7}-Au_{0.3}@CTGU-19	105 s ⁻¹ .g ⁻¹
Ag_{0.6}-Au_{0.4}@CTGU-19	139.5 s ⁻¹ .g ⁻¹
Ag_{0.5}-Au_{0.5}@CTGU-19	64.5 s ⁻¹ .g ⁻¹
Ag_{0.4}-Au_{0.6}@CTGU-19	145 s ⁻¹ .g ⁻¹
Ag_{0.3}-Au_{0.7}@CTGU-19	124.4 s ⁻¹ .g ⁻¹
Ag_{0.2}-Au_{0.8}@CTGU-19	107.6 s ⁻¹ .g ⁻¹
Ag_{0.1}-Au_{0.9}@CTGU-19	124.1 s ⁻¹ .g ⁻¹
Au@CTGU-19	9.56 s ⁻¹ .g ⁻¹

Table S4. The catalytic activity of 0.2 mg composite catalyst for 4-NP reduction reaction.

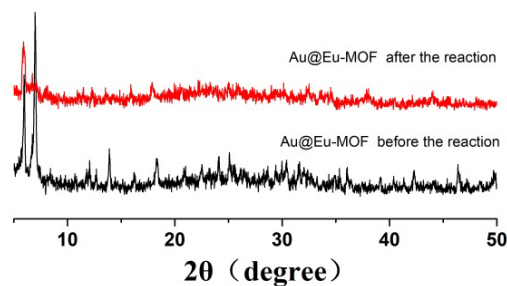
Ag@CTGU-19	164.5 s ⁻¹ .g ⁻¹
Ag_{0.9}-Au_{0.1}@CTGU-19	142 s ⁻¹ .g ⁻¹
Ag_{0.8}-Au_{0.2}@CTGU-19	193.5 s ⁻¹ .g ⁻¹
Ag_{0.7}-Au_{0.3}@CTGU-19	225.5 s ⁻¹ .g ⁻¹
Ag_{0.6}-Au_{0.4}@CTGU-19	220 s ⁻¹ .g ⁻¹
Ag_{0.5}-Au_{0.5}@CTGU-19	257.5 s ⁻¹ .g ⁻¹
Ag_{0.4}-Au_{0.6}@CTGU-19	156.5 s ⁻¹ .g ⁻¹
Ag_{0.3}-Au_{0.7}@CTGU-19	212.5 s ⁻¹ .g ⁻¹
Ag_{0.2}-Au_{0.8}@CTGU-19	141.5 s ⁻¹ .g ⁻¹
Ag_{0.1}-Au_{0.9}@CTGU-19	138.5 s ⁻¹ .g ⁻¹
Au@CTGU-19	64.5 s ⁻¹ .g ⁻¹

Table S5. Catalytic activity of composite catalyst for 4-NP reduction reaction.

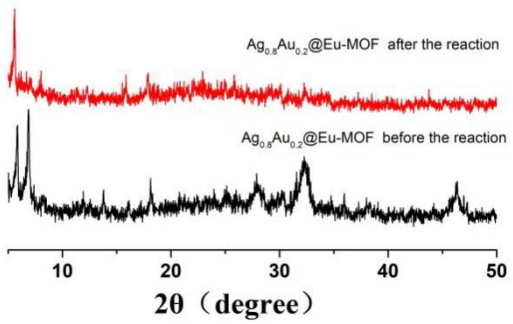
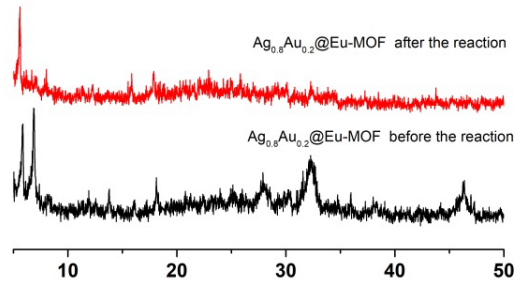
Ag@CTGU-19	19.04 s ⁻¹ .g ⁻¹
Ag_{0.9}-Au_{0.1}@CTGU-19	21.90 s ⁻¹ .g ⁻¹
Ag_{0.8}-Au_{0.2}@CTGU-19	52.34 s ⁻¹ .g ⁻¹
Ag_{0.7}-Au_{0.3}@CTGU-19	24.80 s ⁻¹ .g ⁻¹
Ag_{0.6}-Au_{0.4}@CTGU-19	32.60 s ⁻¹ .g ⁻¹
Ag_{0.5}-Au_{0.5}@CTGU-19	33.40 s ⁻¹ .g ⁻¹
Ag_{0.4}-Au_{0.6}@CTGU-19	33.90 s ⁻¹ .g ⁻¹
Ag_{0.3}-Au_{0.7}@CTGU-19	28.90 s ⁻¹ .g ⁻¹
Ag_{0.2}-Au_{0.8}@CTGU-19	20.60 s ⁻¹ .g ⁻¹
Ag_{0.1}-Au_{0.9}@CTGU-19	33.86 s ⁻¹ .g ⁻¹
Au@CTGU-19	30.32 s ⁻¹ .g ⁻¹



(a)



(b)



(c)

Figure S13. PXRD of (a) $\text{Ag}@\text{CTGU-19}$; (b) $\text{Au}@\text{CTGU-19}$; (c) $\text{Ag}_{0.8}\text{-Au}_{0.2}@\text{CTGU-19}$ before and after nitrophenol reduction experiment.

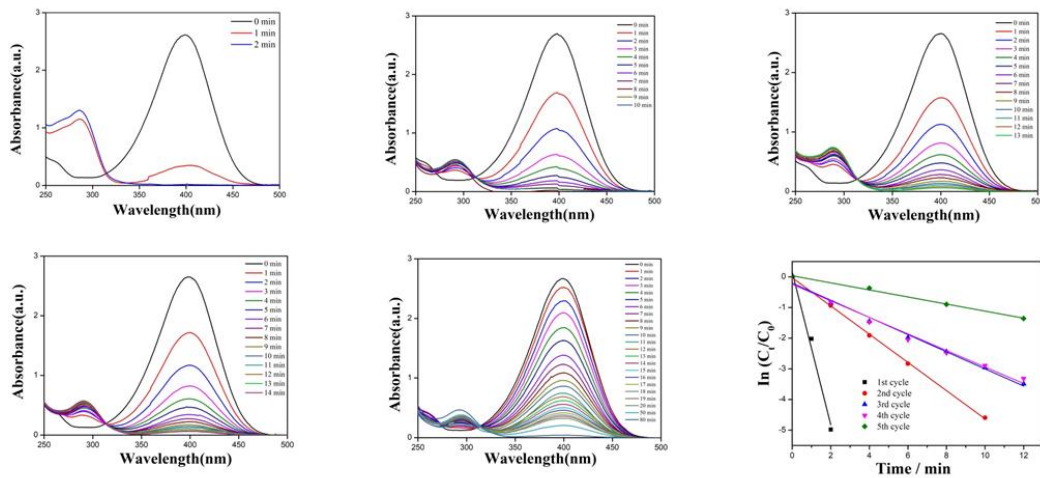


Figure S14. Five cycles of $\text{Ag}_{0.8}\text{-Au}_{0.2}\text{@CTGU-19}$ reduction of 4-NP.

Table S6. Summary of rate constants of other similar 4-nitrophenol reduction reactions catalyzed by previously reported catalysts

Name of Catalyst	reaction rate constants per unit mass ($\text{s}^{-1} \text{ g}^{-1}$)	Reference
CuO-Ag	6.40	(1)
Au/ZSBA-PL	2.36	(2)
Au@S-CLLCS	2.30	(3)
Au NPs	0.51	(4)
Au-Pd/clay	13.66	(5)
Pt@OMS	3.53	(6)
Pt-in-ANTs	13.3	(7)
Ag@CTGU-3	8.64	(8)
Ag@CTGU-4	3.03	(8)
Ag@CTGU-1	25.7	(9)
$\text{Ag}_{0.8}\text{-Au}_{0.2}\text{@CTGU-19}$	52.34	This work

Table S7. Summary of rate constants of other similar 2-nitrophenol reduction reactions catalyzed by previously reported catalysts

Name of Catalyst	reaction rate constants per unit mass ($s^{-1} g^{-1}$)	Reference
Cu/CS-CMM	6	(10)
Fe ₃ O ₄ /SiO ₂ @Ag	5.5	(11)
Au NPs	53	(12)
Au@ CTGU-3	3.33	(8)
Au@ CTGU-4	0.85	(8)
Ag/Au NPs	0.55 (s^{-1})	(13)
Ag _{0.8} -Au _{0.2} @ CTGU-19	68.80	This work

Table S8. Summary of rate constants of other similar 3-nitrophenol reduction reactions catalyzed by previously reported catalysts

Name of Catalyst	reaction rate constants per unit mass ($s^{-1} g^{-1}$)	Reference
Ag@AuNPs	0.69 (s^{-1})	(13)
Colloidal Au NPs	7.33	(14)
Au@ CTGU-3	4.5	(8)
Au@ CTGU-4	1.58	(8)
Colloidal Pt-NPs	3.2 (s^{-1})	(15)
Ag _{0.8} -Au _{0.2} @ CTGU-19	53.60	This work

References

- (1) A. K. Sasmal, J. Pal, R. Sahoo, P. Kartikeya, S. Dutta, and T. Pal, *J. Phys. Chem. C.*, 2016, **120**, 21580.
- (2) D. W. Gao, X. Zhang, X. P. Dai, Y. C. Qin, A. J. Duan, Y. B. Yu, H. Y. Zhuo, H. R. Zhao, P. F. Zhang, Y. Jiang, J. M. Li and Z. Zhao, *Nano Res.*, 2016, **9**, 3099.

- (3) M. Y. Liu, L. B. Wang, R. L. Huang, Y. J. Yu, R. X. Su, W. Qi and Z. M. He, *Langmuir*, 2016, **32**, 10895.
- (4) R. L. Lawrence, B. Scola, Y. Li, C. K. Lim, Y. Liu, P. N. Prasad, M. T. Swihart and M. R. Knecht, *ACS Nano*, 2016, **10**, 9470.
- (5) D. Varadea and K. Haraguchi, *Chem. Commun.*, 2014, **50**, 3014.
- (6) X. C. Liu, D. S. Chen, L. Chen, R. X. Jin, S. X. Xing, H. Z. Xing, Y. Xing and Z. M. Su, *Chem. Eur. J.*, 2016, **22**, 9293.
- (7) M. H. Wang, Z. Gao, B. Zhang, H. M. Yang, Y. Qiao, S. Chen, H. B. Ge, J. K. Zhang and Y. Qin, *Chem. Eur. J.*, 2016, **22**, 8438.
- (8) X. Q. Wu, D. D. Huang, Z. H. Zhou, W. W. Dong, Y. P. Wu, J. Zhao, D. S. Li, Q. C. Zhang and X. H. Bu, *Dalton Trans.*, 2017, **46**, 2430.
- (9) G. W. Xu, Y. P. Wu, W. W. Dong, J. Zhao, X. Q. Wu, D. S. Li and Q. C. Zhang, *Small*, 2017, **13**, 1602996.
- (10) S. Haidera, T. Kamalbc, S. B. Khanbc, M. Omerd, A. Haidere, F. U. Khanbc and A. M. Asiribc, *Appl. Surf. Sci.*, 2016, **387**, 1154.
- (11) K. S. Shin, Y. K. Cho, J. Y. Choi and K. Kim, *Appl. Catal. A: Gen.*, 2012, **413**, 170.
- (12) W. L. Shen, Y. Y. Qu, X. F. Pei, X. W. Zhang, Q. Ma, Z. J. Zhang, S. Z. Li and J. T. Zhou, *Biotechnol. Lett.*, 2016, **381**, 1503.
- (13) L. d. Xu, M. Hong, Y. L. Wang, M. Li, H. B. Li, M. P. N. Nairb and C. Z. Li, *Sci. Bull.*, 2016, **61**, 1525.
- (14) R. Majumdar, B. G. Bag and Pooja Ghosh, *Appl Nanosci.*, 2016, **6**, 521.
- (15) P. Dauthal and M. Mukhopadhyay, *J. Ind. Eng. Chem.*, 2015, **22**, 185.